LA-UR -86-1420

RECEIVED BY OSTI MAY 12 1986

CONF-8603107--4

Los Alamos National Laboratory is operated by the University of California for the United States Department of Energy under contract W-7405-ENG-36

LA-UR--86-1420

DE86 010201

TITLE Gain Physics of Rf-linac-Driven XUV Free-Electron Lasers

AUTHOR(S) John C. Goldstein
Brian D. McVey
Brian E. Newnan

SUBMITTED TO Proceedings of the Third Topical Meeting on Short Wavelength Coherent Radiation: Generation and Application held in Monterey, CA, March 24-26, 1986

DISCLAIMER

MASTER

Los Alamos Los Alamos National Laboratory
Los Alamos, New Mexico 87545

GAIN PHYSICS OF Rf-LINAC-DRIVEN XUV FREE-ELECTRON LASERS*

John C. Goldstein, Brian D. McVey, and Brian E. Newnam
University of California, Los Alamos National Laboratory
Los Alamos, New Mexico 87545 USA

ABSTRACT

In an rf-linac-driven XUV free-electron laser oscillator, the gain depends on the details of the shape of the electron beam's phase-space distribution, particularly the distribution of electrons in the transverse (to the direction of propagation) position and velocity coordinates. This strong dependence occurs because the gain in this device is inhomogeneously broadened. Our previous theoretical studies have assumed that the transverse phase space distribution is a product of uncorrelated Gaussian functions.

In the present work, we shall present the results of a theoretical study of the gain for non-Gaussian phase-space distributions. Such distributions arise either from a better representation of the electron beam from an rf-linac or from an emittance filter applied to the beam after the linac.

INTRODUCTION

In several previous theoretical studies[1,2,3] we have investigated the properties of a free-electron laser (FEL), operating in the extreme ultraviolet (XUV, 10-100 nm) portion of the optical spectrum, which is driven by an electron beam produced by a radio-frequency linear accelerator. The primary problem to be overcome by any FEL oscillator operating in this spectral region is the necessity of achieving large small-signal gain values (at least several hundred percent) in order to exceed the threshold of laser oscillation in an optical resonator with relatively poor reflectors. Mirror reflectances of 50%-80% are expected to become available in the XUV spectral range.[4,5] Extrapolations from presently available accelerator technology suggest that both rf-linacs and electron storage rings can generate pulses of high-energy electrons having sufficiently large peak currents to drive XUV FELs. However, one expects that electron pulses from an rf-linac will have a larger emittance (i.e., occupy a larger volume in phase-space) than those from a storage ring in which synchrotron radiation effects reduce the emittance. A direct consequence is that the gain of an rf-linac-driven XUV FEL will be severely inhomogeneously broadened. Nonetheless, our previous theoretical studies [1,2,3] indicate that sufficient gain will be available to allow for laser oscillation and that an rf-linac-driven XUV FEL would exceed by 4 or 5 orders of magnitude the light intensity in this spectral range available from present or

*Work performed under the auspices of, and supported by, the Division of Advanced Energy Projects of the U.S. Department of Energy, Office of Basic Energy Sciences.

planned synchrotron sources. Other points related to the design and operation of an rf-linac-driven XUV FEL are discussed in the paper by Newnam et al. in these proceedings.

This paper presents the results of a theoretical investigation of the dependence of the magnitude of the small signal gain of an rf-linac- driven XUV FEL upon the shape of the distribution that leads to the inhomogeneous broadening. It is analogous to changing the distribution of atomic velocities in a low-pressure Doppler-broadened gas laser from a Maxwellian to other distribution functions. In a gas, the Maxwellian is the unique physically important distribution; there can be many different distributions in the case of an electron beam. The "correct" distribution function of electrons' transverse motion depends upon details of the design and operation of a linear accelerator and is not known a priori. In an FEL, the magnitude of the transverse emittance determines the amount of inhomogeneous broadening and, therefore, the accompanying reduction of the small- signal gain, much like the value of the temperature determines the amount of Doppler broadening in a low-pressure gas laser. However, the physics of an rf-accelerator allows the possibility of generating electron beams with the same value of the transverse emittance but having different underlying distributions of transverse particle motion. The dependence of the gain upon different distributions, each one having the same value of the emittance, is the subject of this study.

This problem is of some importance because our previous studies[2,3] have assumed that the transverse phase-space distribution of the electron beam is a product of uncorrelated Gaussian functions. The inhomogeneous broadening reduces the gain from very large values (thousands) for a perfect (zero emittance) electron beam to about ten for a beam with a finite emittance. We would like to assure ourselves that the gain is not reduced further through a dependence on the shape of the phase-space distribution. Also, it is important to quantitatively understand the reduction of small-signal gain due to the inhomogeneous broadening in order to place realistic limits on other parameters (such as the peak current, intrinsic energy spread, and wiggler length) in order to assure sufficiently large gain for the laser to exceed threshold with the available mirrors.

TRANSVERSE EMITTANCE

Let $\hat{z}$ be the axis of the optical resonator and the wiggler magnet. The transverse coordinates of an electron are x, x', y, and y' where $x' = dx/dz \simeq \beta_x$ and $y' = dy/dz \sim \beta_y$. We are considering the case of highly relativistic electrons having $\gamma_0 \sim 400$, where $\gamma_0 mc^2$ is the total energy of an electron, for which the transverse velocities $\beta_x c$ and $\beta_y c$ are very small compared to the axial velocity (i.e., $\beta_x, \beta_y \ll 1$). The distribution of electrons in the beam is described by a function $P(x, x', y, y')$, which is normalized to one, such that the current of electrons with coordinates x to x + dx, x′ to x′ + dx′, etc. is given by

$$dI(x, x', y, y') = I_0 P(x, x', y, y')\, dx \qquad (1)$$

Here $d\tau = dx\, dx'\, dy\, dy'$ and I_e is the total current. The mean value of any function $f(x, x', y, y')$ of the transverse variables is given by $\langle f \rangle = \int d\tau P f$. We think of electron trajectories in which the transverse coordinates are functions of the axial coordinate z.

We shall use the definition of Fraser et al[6] for the transverse emittance:

$$\epsilon_x = 4\pi \left[\langle x^2 \rangle \langle x'^2 \rangle - \langle x\, x' \rangle^2 \right]^{1/2} \tag{2}$$

$$\epsilon_y = 4\pi \left[\langle y^2 \rangle \langle y'^2 \rangle - \langle y\, y' \rangle^2 \right]^{1/2} \tag{3}$$

$$\epsilon = \sqrt{\epsilon_x \epsilon_y} \tag{4}$$

In what follows below, we will assume that $\epsilon_x = \epsilon_y = \epsilon$ and we will calculate small-signal gain values for an XUV FEL driven by electron beams having the same total current I_e and emittance ϵ but having different phase-space distribution functions P.

We shall restrict our attention to a particular class of distributions P. Let us define B by

$$B = (x - \bar{x})^2 + (x' - \bar{x}')^2 + (y - \bar{y})^2 + (y' - \bar{y}')^2 \tag{5}$$

where $\bar{x}, \bar{x}', \bar{y}$, and $\bar{y}'$ are fixed constants. We shall only consider distributions P of the form

$$P = P(B) \tag{6}$$

We shall assume that our FEL has an untapered parabolic-pole-face[7] wiggler magnet. Such a wiggler magnet, with equal focusing in x and y, induces electrons to make harmonic oscillations in the transverse variables. The wavenumber of these betatron oscillations is k_β:

$$k_\beta = \frac{a_w k_w}{(2\gamma_0)} \tag{7}$$

where $k_w = 2\pi/\lambda_w$, λ_w is the wavelength of the constant-period wiggler magnet, and

$$a_w = \frac{|e| B_w}{(mc^2 k_w)} \tag{8}$$

where B_w is the peak on-axis value of the magnetic field of the wiggler.

Since the transverse motion of an electron is simple harmonic with wavenumber k_β (neglecting the wiggle motion itself which is the source of the basic FEL mechanism), one can show that if the following matching conditions are satisfied, the form of the function P(B) is the same anywhere inside the wiggler: that is, for any two values of z inside the wiggler, say z_1 and z_2, P $(B(z_1))$ = P $(B(z_2))$. Again, this neglects high-frequency variations due to the wiggle motion itself. The matching conditions connect the four constant parameters of P:

$$x' = k_\beta x \tag{9}$$

$$y' = k_\beta y \tag{10}$$

Since, under these conditions, the fundamental form of P is invariant anywhere inside the wiggler, so is any mean value calculated from P such as the electron beam dimensions $\langle x^2 \rangle$, $\langle y^2 \rangle$, and $\langle r^2 \rangle = \langle x^2 \rangle + \langle y^2 \rangle$.

FOUR SPECIFIC TRANSVERSE PHASE-SPACE DISTRIBUTIONS

We will consider the following four distribution functions which are functions of the transverse coordinates through the variable B which is defined by Eq. (5).

Case 1: Gaussian

$$P_1 d\tau = N \exp(-B) d\tau \tag{11}$$

Case 2: "Almost Gaussian"

$$P_2 d\tau = 1.67097 N \exp(-B^{1.5}) d\tau \tag{12}$$

Case 3: "Almost Uniform"

$$P_3 d\tau = 2.25305 N \exp(-B^4) d\tau \tag{13}$$

Case 4: Uniform

$$P_4 d\tau = 2N d\tau \tag{14}$$

for all values of x, x', y, and y' that lie within the four-dimensional ellipsoidal surface defined by $B = 1$.

The factor N is a normalization factor:

$$N = (\pi^2 x\, x'\, y\, y')^{-1} \tag{15}$$

We exhibit explicitly for these four distributions expressions for the emittance. Let Z ($\bar{Z}$) refer to any of the four quantities x, x', y, y' ($\bar{x}$, $\bar{x}'$, $\bar{y}$, $\bar{y}'$).

Case 1: Gaussian

$$\langle Z^2 \rangle = 0.5 \bar{Z}^2 \tag{16}$$

$$\epsilon_x = 2\pi\ \bar{x}\ \bar{x}';\quad \epsilon_y = 2\pi\ \bar{y}\ \bar{y}' \tag{17}$$

Case 2: Almost Gaussian

$$\langle Z^2 \rangle = 0.278\bar{Z}^2 \tag{18}$$

$$\epsilon_x = 1.1122\pi\ \bar{x}\ \bar{x}';\quad \epsilon_y = 1.1122\pi\ \bar{y}\ \bar{y}' \tag{19}$$

Case 3: "Almost Uniform"

$$\langle Z^2 \rangle = 0.17175\bar{Z}^2 \tag{20}$$

$$\epsilon_x = 0.687\pi\ \bar{x}\ \bar{x}';\quad \epsilon_y = 0.687\pi\ \bar{y}\ \bar{y}' \tag{21}$$

Case 4: Uniform

$$Z^2 = (1/6)\ Z^2 \tag{22}$$

$$\epsilon_x = (2/3)\pi\ x\ x';\quad \epsilon_y = (2/3)\pi\ y\ y' \tag{23}$$

In the numerical examples below, we will always assume that $\epsilon_x = \epsilon_y = \epsilon$. Hence, specifying ϵ, together with the matching conditions Eqs. (9) and (10) is sufficient to fully determine the four parameters of each distribution function.

EFFECTIVE ENERGY DISTRIBUTION FUNCTION

The effects upon FEL performance of a beam with a finite transverse emittance can be understood in terms of the shape of the associated effective energy distribution.[2,3] If one has a monoenergetic beam in which each electron has energy $\gamma_0 mc^2$ but also has a nonzero transverse motion, then to the FEL the electron behaves as if it had an energy $\gamma_{eff}mc^2$ where γ_{eff} is given by

$$\gamma_{eff} = \gamma_0\left[\frac{1 + 0.5\ a_w^2}{1 + 0.5\ a_w^2 + \gamma_0^2\left[\beta_x^2 + \beta_y^2 + (k_\beta x)^2 + (k_\beta y)^2\right]}\right]^{1/2} \tag{24}$$

Here the electron's transverse coordinates and velocities are x, y and $\beta_x c, \beta_y c$, and k_β and a_w are given by Eqs. (7) and (8). Physically, the FEL resonance is a relation between the wiggler magnet properties, the optical wavelength, and the electron's axial velocity. In a beam with a finite emittance, an electron's axial velocity is reduced if it has a finite transverse motion. This reduction is expressed by using γ_{eff} instead of γ_0 in the FEL equations of motion.

Note that given a distribution of transverse coordinates P, we can uniquely obtain an associated distribution of γ_{eff}, $f(\gamma_{eff})$. Also, our selection of a class

of distributions P which can be matched to the wiggler means that $f(\gamma_{eff})$ is the same anywhere within the wiggler, as is P (this of course is true for uniform wiggler magnets whose characteristics do not depend on the longitudinal position z of an electron, and also holds only if the FEL interaction converts only a small fraction of the electron's initial energy $\gamma_0 mc^2$ into light). Our previous studies[2,3] have shown that, for cases of interest for an XUV FEL, the significance of $f(\gamma_{eff})$ is that the gain is approximately proportional to $df/d\gamma_{eff}$: that is, maximum gain occurs where the slope is largest (and positive), and, therefore, distributions f that have large maximum slopes are desirable in that they lead to large values of the gain.

Another consequence of considering distributions P that can be matched to the wiggler is that, if the beam is not matched, then the distribution $f(\gamma_{eff})$ would be different at different axial positions z along the wiggler. Hence, conceptually, the conditions of peak gain would vary along the wiggler in this nonstationary situation, and it would be much harder to understand the processes that lead to the gain.

The specific distributions of effective energy $f(\gamma_{eff})$ that correspond to the four transverse phase-space distributions P above are shown in Figs. 1-4. The wiggler and electron beam properties used to derive these curves are summarized in Table I. Note that we are considering the electron beam to have zero intrinsic energy spread, that is, to be monoenergetic. From the discussion above, it is clear that one would expect Case 4, the uniform distribution, to yield the highest gain since $f(\gamma_{eff})$ for that case, Fig. 4, has a prominent sharp edge where the slope is very large.

RESULTS OF NUMERICAL SMALL-SIGNAL GAIN CALCULATIONS

We emphasize that the ideas associated with $f(\gamma_{eff})$ are helpful in physically understanding the gain mechanism. However, we have used the 3-D FEL simulation code FELEX[4] to numerically compute the results presented below. In this code, the 3-D particle motion and optical diffraction are handled numerically. FELEX does not directly use the distribution function $f(\gamma_{eff})$ in computing the optical gain. All of the results presented below are single-pass gains, not multiple-pass calculations in which the optical mode shape and the gain are calculated iteratively until a self-consistent solution for both is reached.[3] We assume that the light at the entrance to the wiggler is in the lowest-order Gaussian mode which is specified by a Rayleigh range and an optical wavelength.[2] The amplitude of the optical field is fixed by specification of an initial light intensity. For each value of the Rayleigh range, the optical wavelength is varied to obtain the maximum gain. These are single wavefront calculations which neglect the pulsed nature of the electron and optical beams.

Figure 5 shows the results of numerically calculating the small-signal power gain versus the Rayleigh range of the initial light. The other system parameters

are specified in Table I, and these results are for a 12-m wiggler. The four curves correspond to the four distributions listed above. Note that the dotted curve, which is for Case 4, the uniform distribution, has been reduced in ordinate by a factor of ten. Hence, this case, which gives a maximum gain of about 130 at a Rayleigh range of 600 cm, yields the highest gain of the four cases all of which have the same normalized emittance ($\gamma_o \epsilon = \epsilon_n$) of $39\pi \times 10^{-4}$ cm rad. Note that the highest gain exceeds the lowest gain by almost a factor of ten. Also, note the different dependence on Rayleigh range for the four cases: if one knew that the electron beam was Gaussian, one would need an optical resonator that produced a Rayleigh range of 300 cm, whereas 600 cm is needed if the beam is correctly described by distribution P_4.

Figure 6 shows results for identical conditions but using a 6-m wiggler. The magnitude of the gain is lower than for the 12-m wiggler, but Case 1, the Gaussian, shows the highest gain. Note that the optimum Rayleigh range for each case has also changed. For a simple two-mirror optical resonator with mirrors of fixed radii of curvature, the Rayleigh range can be changed by changing the length of the resonator.[9] However, in an FEL oscillator, the length of the optical resonator is not arbitrary but is closely tied to the time interval between successive electron pulses from the accelerator.[10] Hence, different phase-space distributions can substantially impact the design of the optimum FEL optical resonator.

Figure 7 shows the effect of relaxing one assumption made up to this point: the gain for three different distributions is plotted versus intrinsic fractional energy spread ($\Delta\gamma/\gamma_o$). The transverse emittance is the same as before, but one sees that for large energy spreads $\sim 0.4\%$, all cases look similar (and have substantially depressed gains). In this regime, the physics of the inhomogeneous broadening is totally dominated by the real energy spread of the electron beam, not the emittance. The distribution $f(\gamma_{eff})$ would be almost identical with $f(\gamma)$, the distribution of actual electron energies which in these calculations is taken to be Gaussian in shape about $\gamma_o = 400$. The full width at e^{-1} points is the abscissa of Fig. 7. Evidently the intrinsic energy spread must be held to a few tenths of a percent if this laser is to exceed threshold.

Figure 8 shows the effect of changing the current upon the magnitude of the small-signal gain for two of the phase space distributions only. The upper pair of curves, one solid and one dotted which intersect at a current of 100 A and a gain of 130, are for the uniform distribution, Case 4. The lower pair of curves, which intersect at a current of 100 A and a gain of 32, are for the Gaussian distribution, Case 1. The solid lines show the effect of changing the current while the emittance is held constant. The dotted lines show the effect of keeping the brightness constant: the brightness is proportional to the current divided by the square of the emittance. Hence, for the dotted curves the emittance changes like the square root of the change in current.

We emphasize that the most important parameter in determining the mag-

nitude of the gain is the value of the emittance (whatever the underlying distribution). Looking at the upper pair of curves for the uniform distribution, we see that gain drops by almost a factor of 10 for a $\sqrt{2} - 1 \simeq 40\%$ increase in the emittance at 200 A current.

SUMMARY AND CONCLUSIONS

The dependence of the small-signal gain of an rf-linac-driven XUV FEL upon the shape of the electrons' transverse phase-space distribution function has been studied. Single-pass small-signal gain values were calculated using the three-dimensional FEL simulation code FELEX.[8] A particular class of distribution functions was considered. Electron beams characterized by a distribution belonging to this class can always be matched to the wiggler magnet so that the phase-space distribution, as well as averages computed from it, are invariant with respect to axial position along the magnet's length.

We have found that, for a given value of the emittance, different transverse phase-space distributions can yield substantially different (by factors of three to ten) small-signal gain values. The dependence of the magnitude of the gain upon the Rayleigh range of the incident light is different for different phase-space distributions. This dependence for a Gaussian electron beam shape has been discussed by Colson and Elleaume[11] for low-gain conditions with no inhomogeneous broadening or betatron motion, and fixed lowest-order Gaussian optical mode shape.

We have found that, for the range of other parameters of interest for an rf-linac-drive XUV FEL, the particular distribution that yields the highest gain depends upon the length of the wiggler magnet used. Also, the physical insight provided by the shape of the effective energy distribution $f(\gamma_{eff})$ must be supplemented by considerations of the transverse spatial overlap between the electron and light beams. We have not seen strong optical guiding effects[12] in any of these calculations; rather, the optical mode is distorted from that of free-space propagation. Hence, we use optical beam size variations—in the qualitative arguments below—based upon free-space propagation mode sizes. In free space, the mean squared optical mode radius $\langle w^2 \rangle$ averaged over the wiggler length for a mode focused at the middle of the wiggler can be written as

$$\langle w^2 \rangle = \left(\frac{\lambda}{\pi}\right)\left[RR + (L_w/2)^2/(3RR)\right] \tag{25}$$

where L_w is the wiggler length, RR is the Rayleigh range, and λ is the optical wavelength. For a fixed L_w, the minimum $\langle w^2 \rangle$ occurs for $RR = L_w/(2\sqrt{3})$. In that case

$$\langle w^2 \rangle_{min} = \lambda\, L_w/\pi\sqrt{3} \tag{26}$$

The results of Figs. 5 and 6 show that maximum gain for Case 1, the Gaussian phase-space distribution, is achieved under approximately this condition. On

the other hand, maximum gain for Case 4, the uniform distribution, is attained for large values of $\langle w^2 \rangle$ where Eq. (25) reduces approximately to

$$\langle w^2 \rangle \simeq \frac{\lambda}{\pi} RR \tag{27}$$

i.e., the Rayleigh range is large and $\langle w^2 \rangle$ is approximately independent of the wiggler length. We note that the physical-space current densities corresponding to Case 1 and Case 4, obtained from $J(x,y) = I_o \int dx' dy' P$, are

$$J_1 = (2k_\beta I_o/\epsilon) \exp\left(- \left[(x/\bar{x})^2 + (y/\bar{y})^2 \right] \right) \tag{28}$$

$$J_4 = (4k_\beta I_o/3\epsilon) \left[1 - (x/\bar{x})^2 - (y/\bar{y})^2 \right] \tag{29}$$

so that the Gaussian case has a higher current density on axis than the uniform case by 50% for the same emittance:

$$J_4(0.0)/J_1(0.0) = 0.67 \tag{30}$$

Hence, for small optical spot sizes $\langle w^2 \rangle$, the Gaussian has the higher gain. The electrons that contribute to the sharp edge of Fig. 4, $f(\gamma_{eff})$ for the uniform distribution, have a large transverse energy, since $\gamma_{eff} \approx \gamma_o$ – Const. · (transverse energy). Those electrons clearly lie near the surface of the ellipse B = 1 and are in some sense on the "outside" of the real-space current density J_4. In order for those electrons to be effective in generating gain, there must be light at large radius, and so maximum gain in this case occurs for large $\langle w^2 \rangle$. The fact that Case 4 gives the highest gain for a long wiggler, but not for the shorter wiggler, may be connected with the finite "delay length" needed before exponential gain becomes apparent; Case 1 may never be in the exponential gain regime. Note that the variation with wiggler length of the gain is also different for the four cases.

As pointed out in Ref. 11, the small-signal power gain curves of Figs. 5 and 6 roll off at large Rayleigh range because the energy extracted from the electron beam, with a fixed on-axis intensity of light at the wiggler's entrance, becomes smaller relative to the total power in the light beam due to the increased optical beam transverse dimension with increasing Rayleigh range. The curves roll off at small Rayleigh range due to this effect as well as the rapid phase variation of the light $(\phi \propto \tan^{-1}(z/RR))$ which shifts the light out of resonance with the electron beam. We note that arbitrary values of RR are not allowed since the optical beam must be smaller than the wiggler gap. In our case, this means that $60 \leq RR \leq 1500$ for the 6-m case and $240 \leq RR \leq 1500$ for the 12-m case to avoid severe vignetting at the ends of the wiggler.

Figure 7 shows that intrinsic energy spreads larger than a few tenths of a percent drastically reduce the gain for the cases studied. Recent numerical simulations of the energy spread in a 500 Mev linac using the code PARMELA[13] show that by proper phasing of the rf-fields in accelerator cavities the energy spread can be held to less than 0.1%.

Figure 8 reminds us that, for zero intrinsic energy spread, the dominant property that determines the small-signal gain is the magnitude of the emittance. Figure 8 suggests that the variation of the gain with emittance is different for the four different cases, but we have not yet made such calculations. Also to be done in the future is a study of how the saturated gain varies among these four different transverse phase-space distributions, as well as calculations that extend the results of this paper to other optical wavelengths, i.e., 50 nm and 12 nm. Multiple-pass self-consistent oscillator solutions[3] should be calculated to obtain information about the optical quality of the light beam, and to obtain more accurate values of the small-signal gain particularly in high-gain cases. Finally, we remark that gain calculations using numerically calculated transverse phase-space distributions generated by PARMELA, or some other linear accelerator simulation code, may be done in the future.

ACKNOWLEDGMENT

One of the authors (J.C.G.) thanks Walter P. Lysenko for useful discussions on the numerical generation of arbitrary phase-space distributions.

REFERENCES

1. Brian E. Newnam, John C. Goldstein, John S. Fraser, and Richard K. Cooper, in Free Electron Generation of Extreme Ultraviolet Coherent Radiation, AIP Conference Proceedings, No. 118, J. M. J. Madey and C. Pellegrini, Eds. (American Institute of Physics, N.Y., 1984), p. 190.
2. John C. Goldstein, Brian E. Newnam, Richard K. Cooper, and Jack C. Comly, Jr., in Laser Techniques in the Exteme Ultraviolet, AIP Conference Proceedings Number 119, S. E. Harris and T. B. Lucatorto, Eds. (American Institute of Physics, N.Y., 1984), p. 293.
3. John C. Goldstein, Brian D. McVey, and Brian E. Newnam, in Proceedings of the International Conference on Insertion Devices for Synchrotron Sources held at SLAC Oct. 27-30, 1985, to be published.
4. Troy W. Barbee, Jr., in Reference 1, p. 53.
5. Eberhard Spiller, in Reference 2, p. 312.
6. J. S. Fraser, R. L. Sheffield, E. R. Gray, and G. W. Rodenz, IEEE Tr. on Nucl. Sci. NS – 32, 1791 (1985).
7. E. T. Scharlemann, J. A. P. 58, p. 2154 (1985).
8. Brian D. McVey in Proceedings of the Seventh International Free-Electron Laser Conference held at Tahoe City, Calif., Sept. 8-13, 1985, to be published.

9. H. Kogelnik and T. Li, Proc. IEEE 54, 1312 (1966).
10. W. B. Colson and A. Renieri, J. de Physique 44, Colloque C1, Supplement 2, p. 1 (1983).
11. W. B. Colson and P. Elleaume, Appl. Phys. B. 29, 101 (1982).
12. David A. G. Deacon, John M. J. Madey, and John LaSala, these proceedings.
13. Bruce Carlsten, private communication.

TABLE I
PARAMETER VALUES FOR GAIN CALCULATIONS

Optical Parameters	
a) wavelength	variable, near 82 nm
b) Rayleigh range	variable, 50-1200 cm
Uniform REC Undulator Parameters	
a) wavelength, λw	1.6 cm
b) peak magnetic field, Bw	0.75 T
c) a_w	1.12
d) full gap	0.4 cm
e) length	6-m or 12-m
f) parabolic-pole-face with equal focusing in x and y	
Electron Beam Parameters	
a) peak current	100 A
b) E/mc^2	$\gamma_0 = 400$
c) ϵ	3.0630×10^{-5} cm rad
d) $\epsilon_n = \gamma_0 \epsilon$	39π mm-mrad
e) $\lambda_\beta = 2\pi/k_\beta$	1.143×10^3 cm
f) fractional intrinsic energy spread $\Delta\gamma/\gamma_0$	0

FIGURE CAPTIONS

Figure 1: Effective energy distribution function for Case 1.
Figure 2: Effective energy distribution function for Case 2.
Figure 3: Effective energy distribution function for Case 3.
Figure 4.: Effective energy distribution function for Case 4.
Figure 5.: Small-signal power gain vs. Rayleigh range for 12-m wiggler.
Figure 6: Small-signal power gain vs. Rayleigh range for 6-m wiggler.
Figure 7: Gain reduction caused by intrinsic energy spread.
Figure 8: Variation of gain with current for 12-m wiggler.

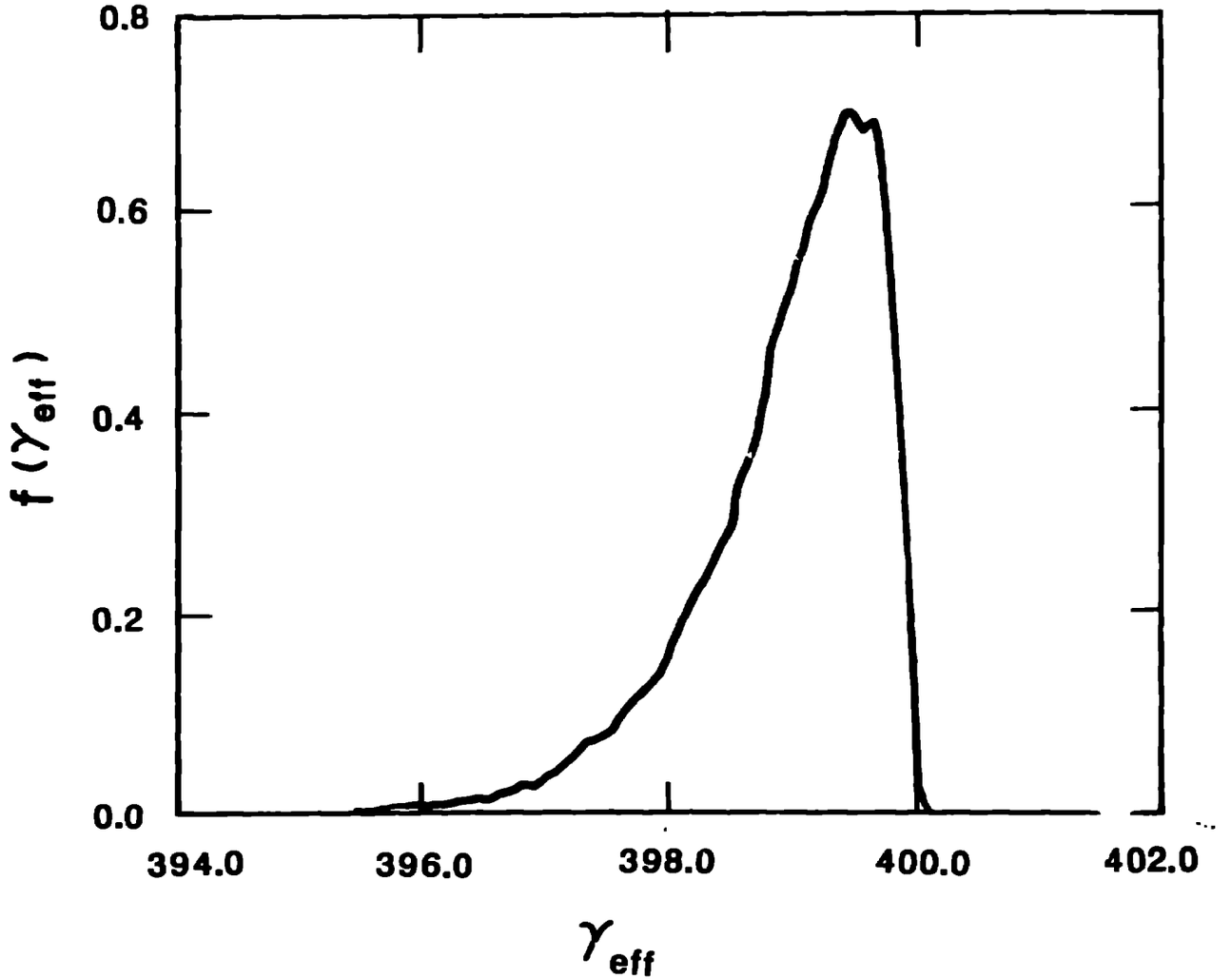
0.8
0.6
0.4
0.2
0.0
f (γeff)
394.0
396.0
398.0
400.0
402.0
γeff

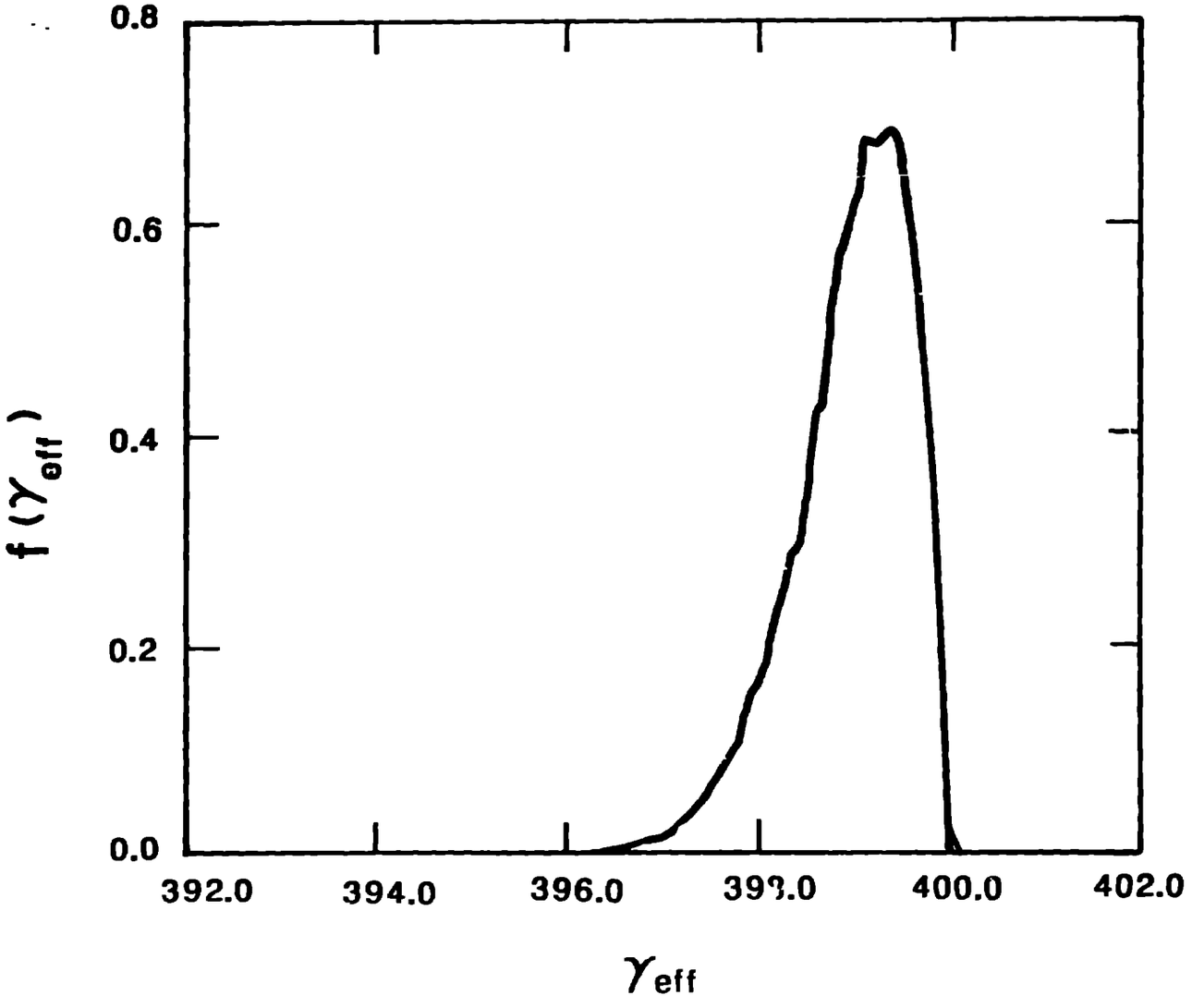
0.8
0.6
0.4
0.2
0.0
f (γeff)
392.0
394.0
396.0
398.0
400.0
402.0
γeff

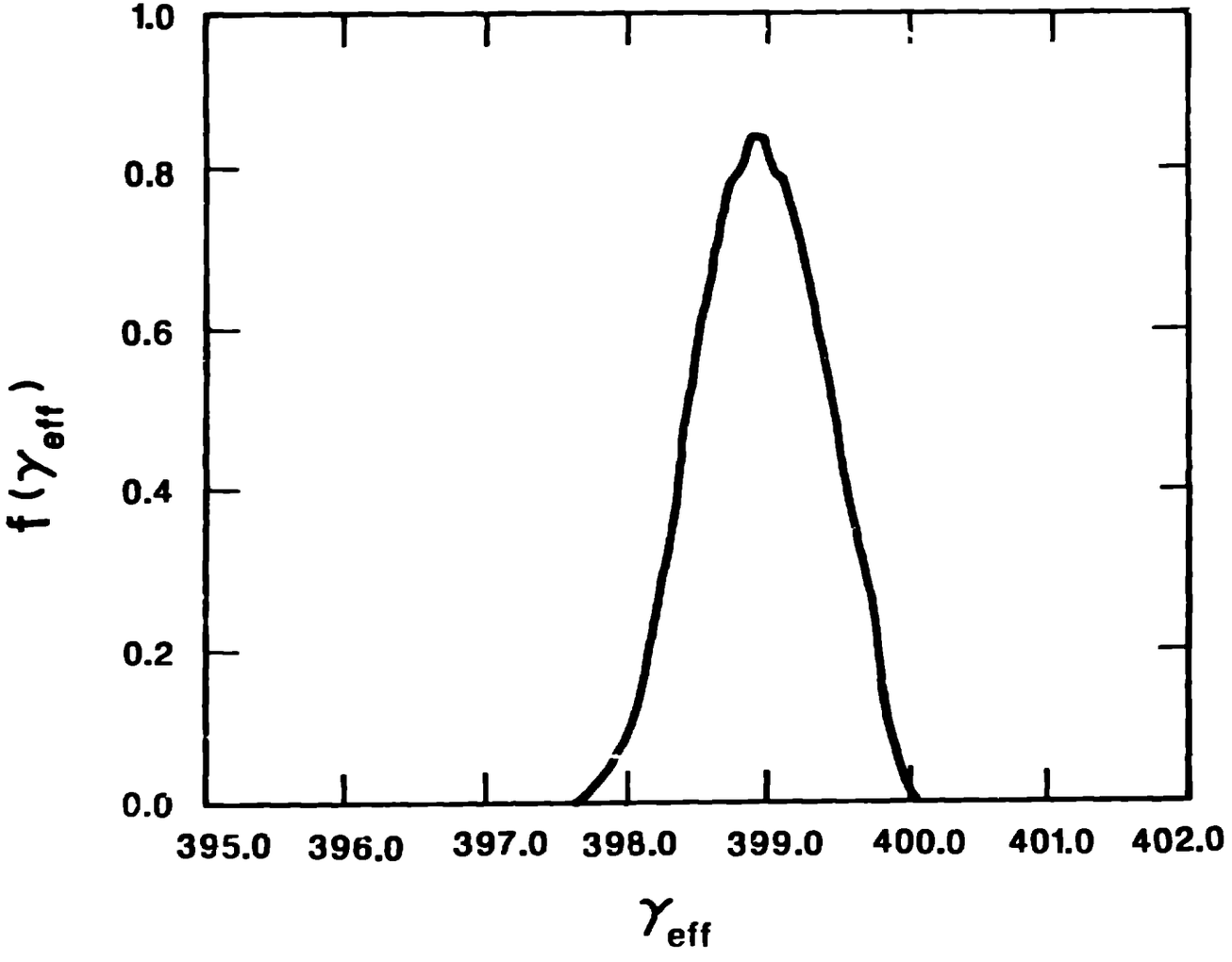
1.0
0.8
0.6
0.4
0.2
0.0
$f(\gamma_{eff})$
395.0
396.0
397.0
398.0
399.0
400.0
401.0
402.0
γ_{eff}

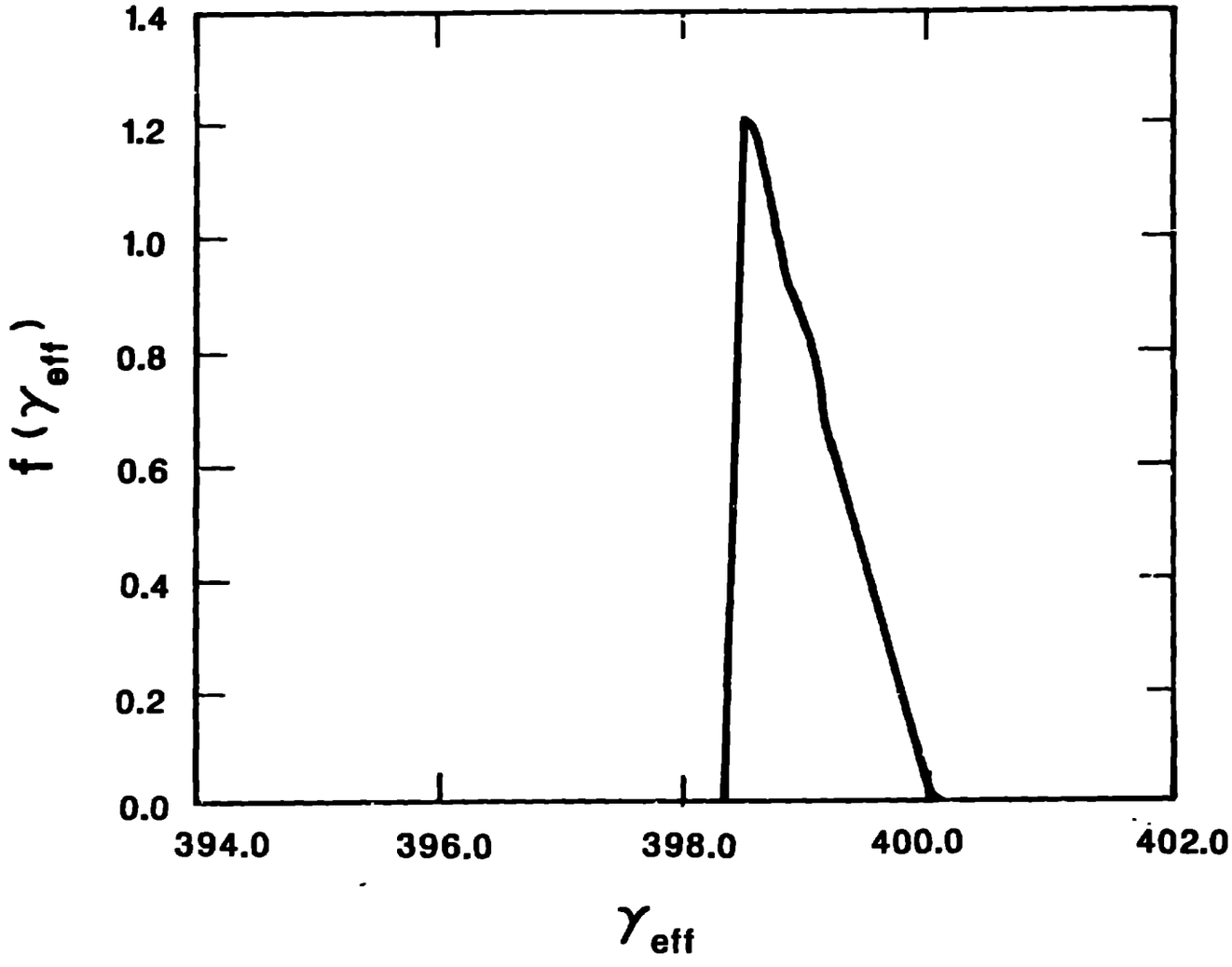
1.4
1.2
1.0
0.8
0.6
0.4
0.2
0.0
f (γeff)
394.0
396.0
398.0
400.0
402.0
γeff

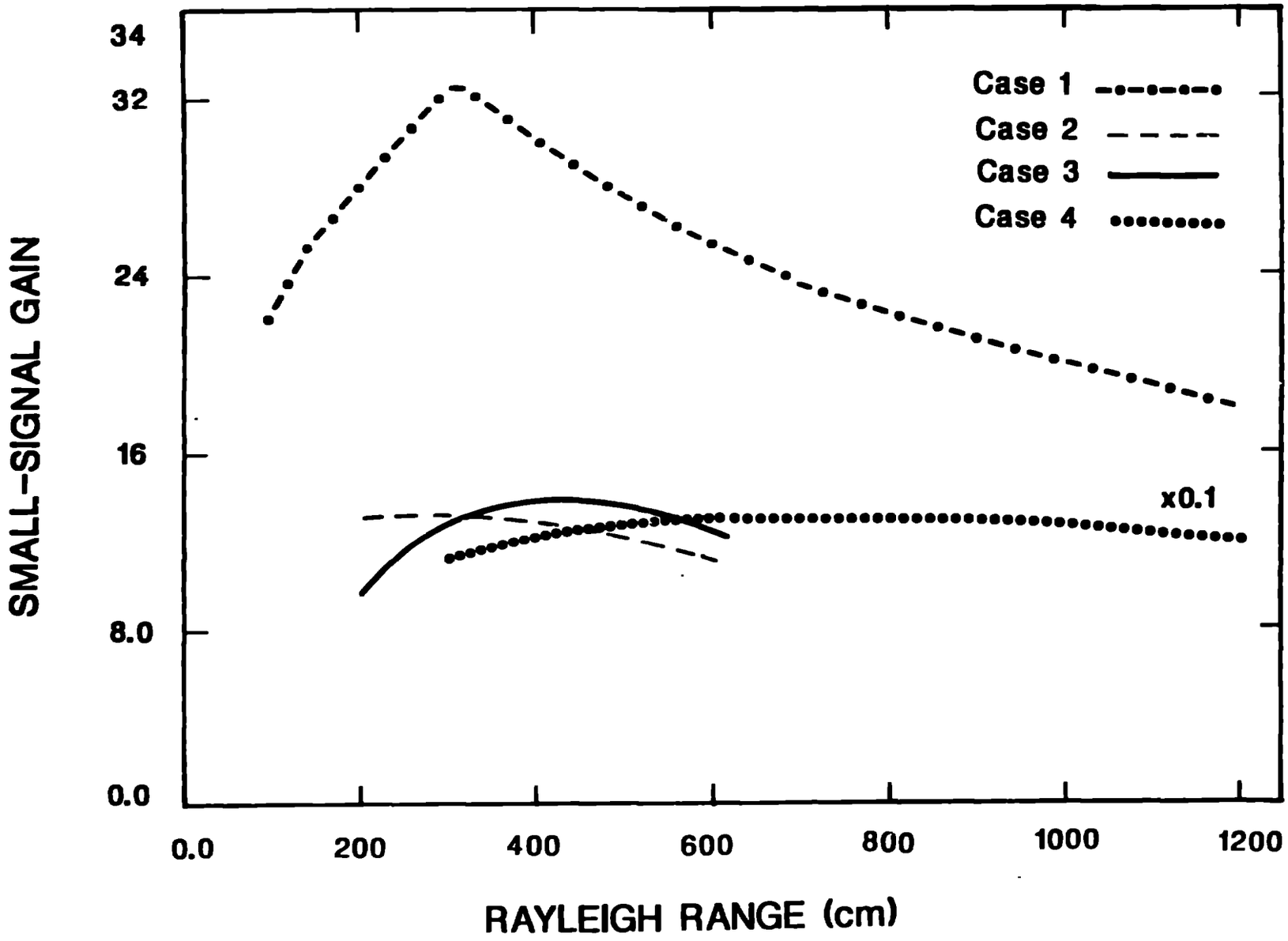
34
32
24
16
8.0
0.0
SMALL-SIGNAL GAIN
Case 1
Case 2
Case 3
Case 4
x0.1
0.0
200
400
600
800
1000
1200
RAYLEIGH RANGE (cm)

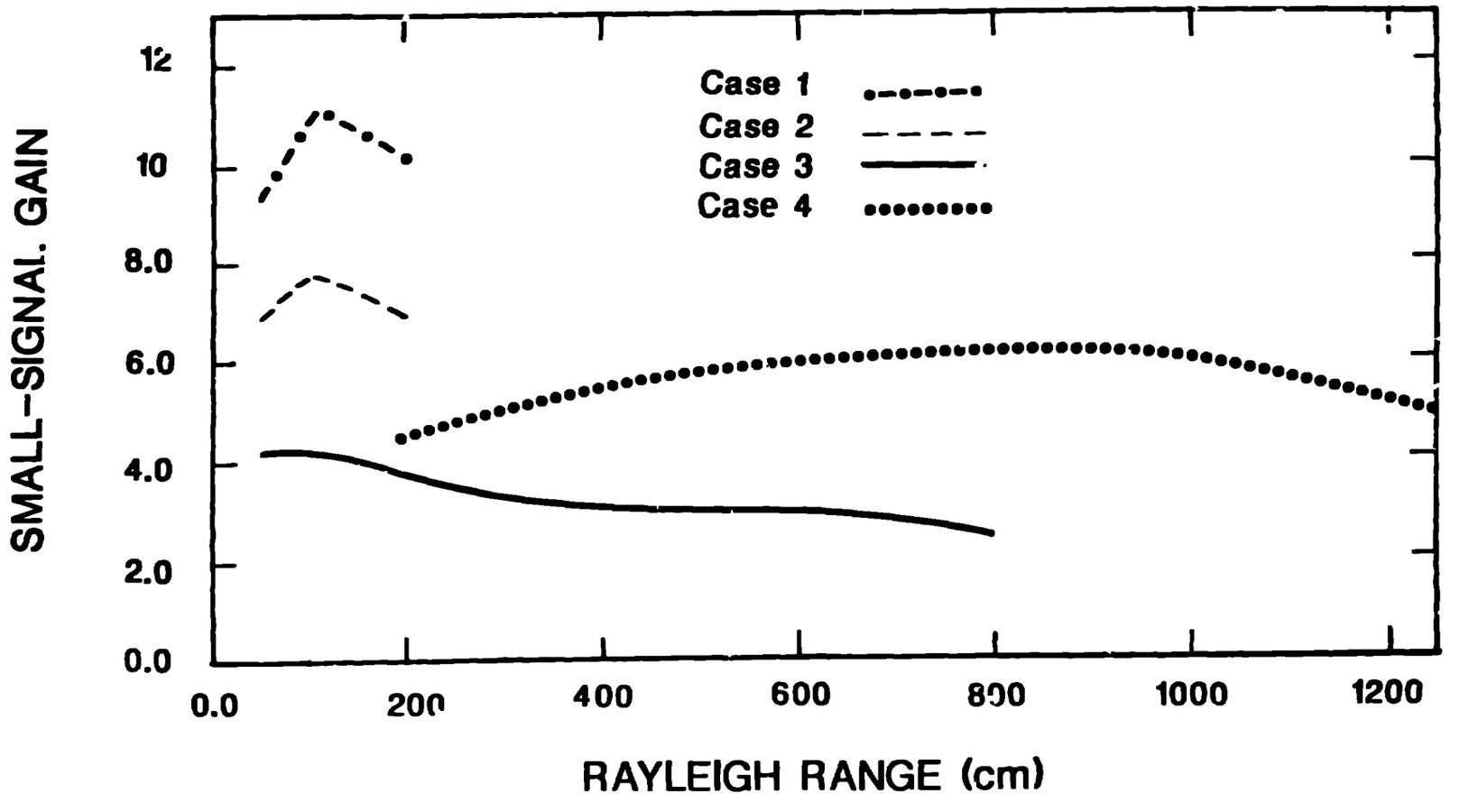
SMALL-SIGNAL GAIN
12
10
8.0
6.0
4.0
2.0
0.0
0.0
200
400
600
800
1000
1200
RAYLEIGH RANGE (cm)
Case 1
Case 2
Case 3
Case 4

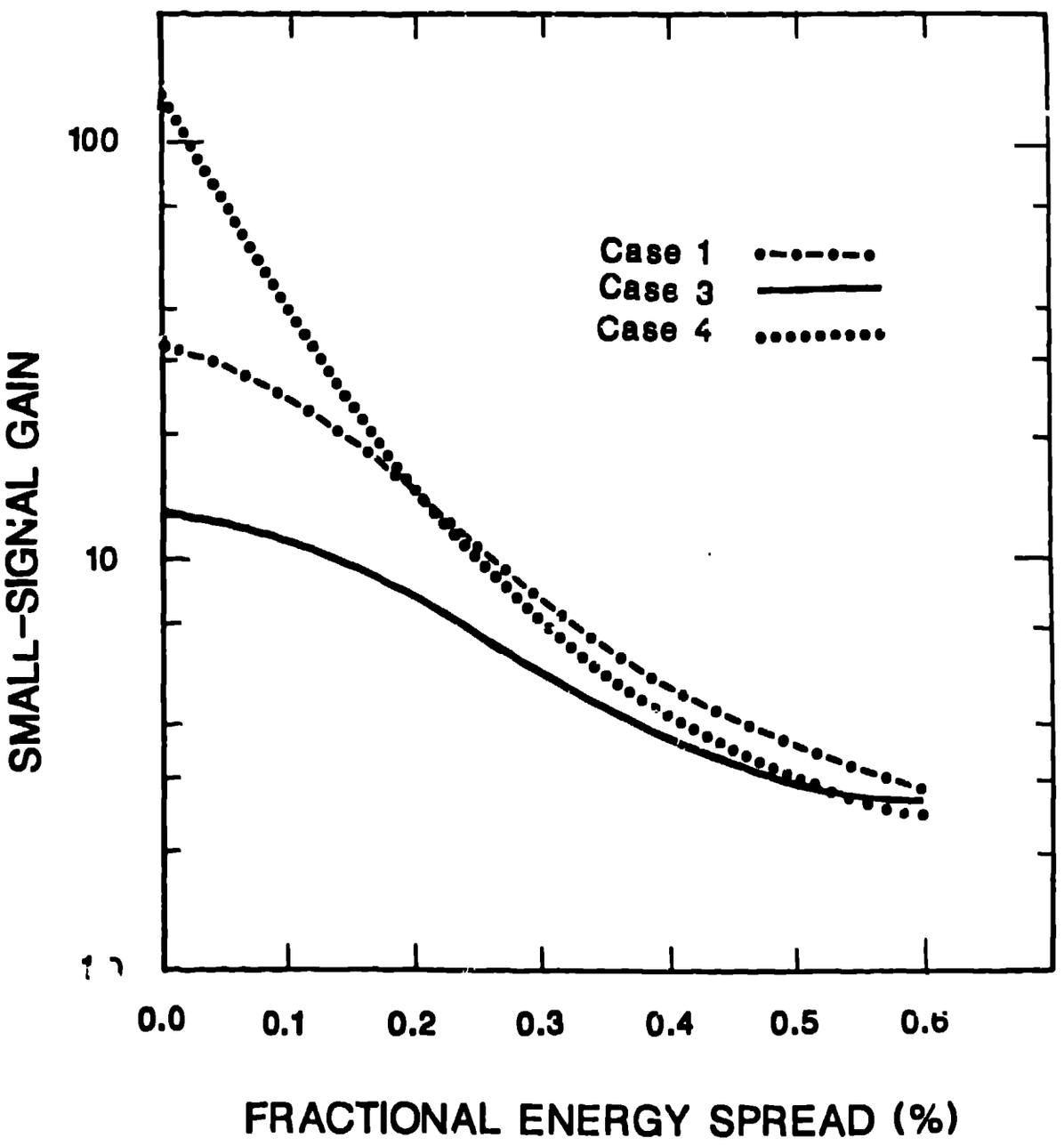
100
10
SMALL-SIGNAL GAIN
Case 1
Case 3
Case 4
0.0
0.1
0.2
0.3
0.4
0.5
0.6
FRACTIONAL ENERGY SPREAD (%)

F.

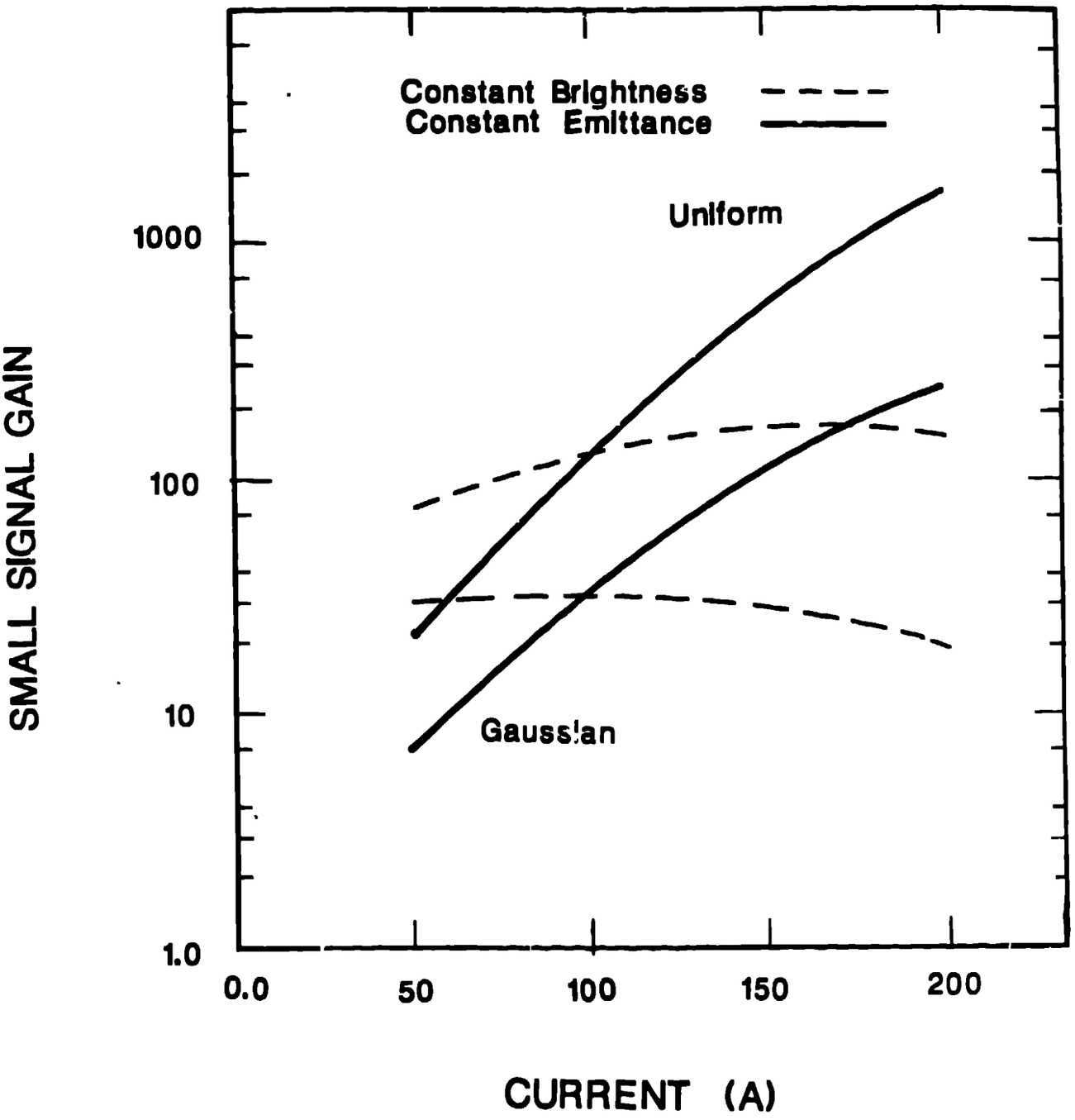
Constant Brightness
Constant Emittance
Uniform
Gaussian
SMALL SIGNAL GAIN
1000
100
10
1.0
0.0
50
100
150
200
CURRENT (A)

Fig. 4